International Journal of Engineering &Technology, 7 (4) (2018) 6851-6855

International Journal of Engineering & Technology

Website: www.sciencepubco.com/index.php/IJET
doi: 10.14419/ijet.v7i4.27100
Research paper

Simulating performance characteristics of induction motor under a balanced load by direct on-line starting

Oti Stephen Ejiofor [1] *, Nwosu Cajethan Abuchi [1], Nnadi Damian Benneth [1], Madueme Victory [1]

[1] Department of Electrical Engineering, University of Nigeria, Nsukka, Enugu State. Nigeria
**Corresponding author E-mail: stephen.oti@unn.edu.ng*

Abstract

This paper divulges the use of MATLAB simulation model to investigate the performance characteristics of a three-phase induction motor using the Direct on-line (DOL) starting. The induction motor operational characteristics by the DOL scheme during transients and start-up periods and afterwards were investigated. The induction motor parameters and the generated equations were expressly used to create the embedded MATLAB functions which in turn were used to engender the graphs for better comprehension.

Keywords: *DOL; Induction; Load; Simulation; Performance.*

1. Introduction

Asynchronous machines are known to be superior to their DC counterparts and most widely used in industries because of their ruggedness, robustness, reliability, low cost, output power per weight, high efficiency and good self-starting capability [1, 2]. The induction machine is used in a wide variety of applications as a means of converting electric power to mechanical work. It is according to [3], without doubt, the workhorse of the electric power industry as pumps, steel mill, and hoist drives are but a few applications of large multiphase induction motors. On a smaller scale, the 2- phase servomotor is used in position-follow-up control systems, and single-phase induction motors are widely used in household appliances as well as in hand and bench tools. The main aspect which distinguishes induction motor from synchronous motors is that induction motors are capable of producing torque at any speed below synchronous speed [4]. The purpose of this work is to run the modelled induction motor, obtain its physical parameters and examine the characteristic performances by examining the phase currents curves, motor speed curve, electromagnetic torque curve and the torque-speed curve of the induction motor using SIMULINK (a tool box extension of the MATLAB program).

2. Asynchronous induction machine

The three-phase induction motors, which are widely used in industrial and commercial applications, are capable of producing torque at any speed below synchronous speed. In [5], a work was carried out on the dynamic simulation of small power induction motor based on mathematical modeling. The dynamic simulation is one of the key steps in the validation of the design process of the motor drive systems and it is needed for eliminating unintended design mistakes and the resulting error in the prototype construction and testing. Akpama, E.J, O.I. Okoro and E. Chikuni [6], presented a work on the simulation of an induction machine performance under an unbalanced source voltage condition. Their analysis compared the performance of the machine under balanced and unbalanced conditions. Munira Batool [7] did a research using mathematical modelling and speed-torque analysis of 3-Φ induction motor using MATLAB/SIMULINK. In his work, he presented the speed-torque characteristics of an induction motor which were calculated on the basis of a mathematical model. This technique is in compliance with the IEEE standard test procedure for polyphase induction rotors and generators. In [8, 9] different works on the induction motor tests using MATLAB/SIMULINK and their integration into electric machinery have also been carried out. The work in [8] describes MATLAB/SIMULINK implementation of three phase induction motor tests, namely; DC, No load, blocked-rotor test performed to identify equivalent circuit parameters. These simulation models were developed to support and improve electric machinery processes bearing in mind that, the voltages obtained from a three-phase system are usually balanced under balanced conditions. The unbalanced phase voltages do exist due to the presence of unbalanced loads on the system or due to some line disturbances [10, 11]. Very often, the supply to an induction motor is deliberately unbalanced to get modified speed torque curves, as in asymmetrical voltage control as applied to cranes [12], though in this case, there will be a reduction in the operating efficiency.

3. Equivalent circuit of three phase induction motor

Mathematical model of an induction motor is usually done in the arbitrary rotating reference frame, from which other reference frames are realized. The two commonly used reference frame are the stationary reference frame and the synchronously rotating reference. The former is realized by substituting the variable $\omega = 0$, and the latter is realized by substituting $\omega = \omega_e$, where ω_e is the synchronous speed of the motor in electrical radians per second. Details of the derivation of the conventional synchronous motor can be found in [13], and the equivalent circuit is shown below:

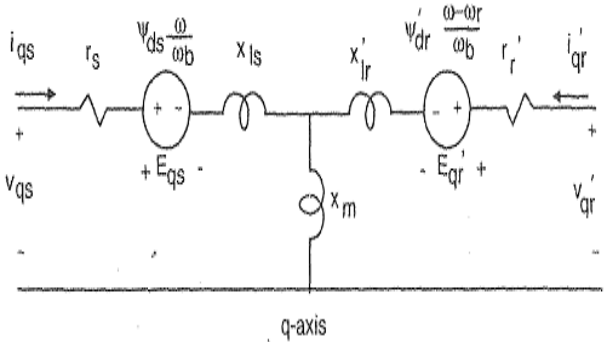

Fig. 1: Q-Axis Equivalent in the Arbitrary Reference Frame.

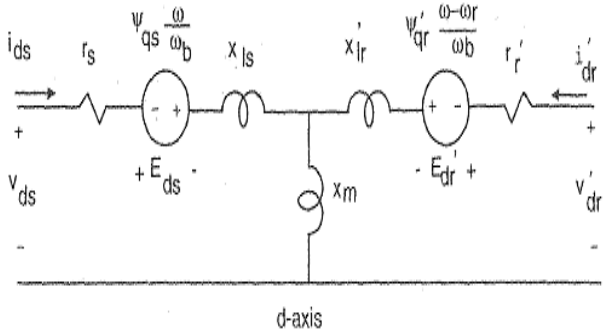

Fig. 2: D-Axis Equivalent in the Arbitrary Reference Frame.

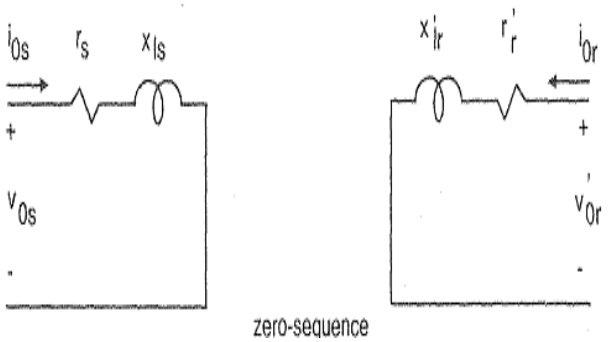

Fig. 3: Zero Sequence Equivalent Circuit.

3.1. Mathematical model of three phase induction motor

Induction motors are seldom simulated in the arbitrary rotating reference frame. In this work, the stationary reference frame was used. The flux linkage equations were scaled by the base speed, ω_b. Usually, induction motor equations are usually expressed in terms of flux linkages per second, Ψ, and reactance, x, instead of flux linkage, λ, and inductance, L. Their relationship is given below:

$$\Psi = w_b \lambda \text{ V} \quad (1)$$

$$x = w_b L \text{ Ohms} \quad (2)$$

The flux linkages per second are given by:

$$\frac{d\Psi_{qs}}{dt} = w_b\left[v_{qs} - \frac{w_e}{w_b}\Psi_{ds} - \frac{r_s}{x_{ls}}(\Psi_{qs} - \Psi_{mq})\right] \quad (3)$$

$$\frac{d\Psi_{ds}}{dt} = w_b\left[v_{ds} + \frac{w_e}{w_b}\Psi_{ds} - \frac{r_s}{x_{ls}}(\Psi_{ds} - \Psi_{md})\right] \quad (4)$$

$$\frac{d\Psi_{0s}}{dt} = w_b\left(v_{0s} - r_s\frac{\Psi_{0s}}{x_{ls}}\right) \quad (5)$$

$$\frac{d\Psi'_{qr}}{dt} = w_b\left[v'_{qr} - \frac{(w_e - w_r)}{w_b}\Psi'_{dr} - \frac{r'_r}{x'_{lr}}(\Psi'_{qr} - \Psi_{mq})\right] \quad (6)$$

$$\frac{d\Psi'_{dr}}{dt} = w_b\left[v'_{dr} + \frac{(w_e - w_r)}{w_b}\Psi'_{qr} - \frac{r'_r}{x'_{lr}}(\Psi'_{dr} - \Psi_{md})\right] \quad (7)$$

$$\frac{d\Psi'_{0r}}{dt} = w_b\left[v'_{0r} - \frac{r'_r}{x'_{lr}}\Psi'_{0r}\right] \quad (8)$$

Let; $$\frac{1}{x_M} = \frac{1}{x_m} + \frac{1}{x_{ls}} + \frac{1}{x'_{lr}} \quad (9)$$

In matrix form equations (3) to (8) is given as (neglecting zero sequence component and noting that the rotor is shorted).

$$\begin{bmatrix} p\Psi_{qs} \\ p\Psi_{ds} \\ p\Psi_{qr} \\ p\Psi_{dr} \end{bmatrix} = \begin{bmatrix} \frac{w_b r_s x^*_{ml}}{x_{ls}(x_{ls}-1)} & -w_e & \frac{w_b r_s x^*_{ml}}{x_{ls}x_{lr}} & 0 \\ w_e & \frac{w_b r_s x^*_{ml}}{(x_{ls}-1)} & 0 & \frac{w_b r_s x^*_{ml}}{x_{ls}x_{lr}} \\ \frac{w_b r_r x^*_{ml}}{x_{ls}x_{lr}} & 0 & \frac{w_b r_r x^*_{ml}}{(x_{lr}-1)} & w_r - w_e \\ 0 & \frac{w_b r_r x^*_{ml}}{x_{ls}x_{lr}} & w_e - w_r & \frac{w_b r_r x^*_{ml}}{x_{lr}(x_{lr}-1)} \end{bmatrix} \begin{bmatrix} \Psi_{qs} \\ \Psi_{ds} \\ \Psi_{qr} \\ \Psi_{dr} \end{bmatrix} + w_b \begin{bmatrix} v_{qs} \\ v_{ds} \\ 0 \\ 0 \end{bmatrix} \quad (10)$$

From the qd0 equivalent circuit of figures 1, 2 and 3, where 'd' is direct axis, 'q' is quadrature axis, 's' is stator variable and 'r ' is rotor variable, v_{qs}, v_{ds}, and v_{0s} are the q-axis, d-axis and zero sequence stator voltages and was obtained by applying the park's transformation on the stator input voltages:

$$[V_{qd0s}] = [T_{qd0}(\theta)][V_{abcs}] \quad (11)$$

$$\begin{bmatrix} V_{qs} \\ V_{ds} \\ V_{0s} \end{bmatrix} = \begin{bmatrix} \frac{2}{3} & -\frac{1}{3} & \frac{1}{3} \\ 0 & -\frac{\sqrt{3}}{3} & \frac{\sqrt{3}}{3} \\ \frac{1}{3} & \frac{1}{3} & \frac{1}{3} \end{bmatrix} \begin{bmatrix} V^s_{as} \\ V^s_{bs} \\ V_{0s} \end{bmatrix} \quad (12)$$

Where $$[T_{qd0}(\theta)] = \frac{2}{3}\begin{bmatrix} cos\theta & \cos(\theta - 2\pi/3) & \cos(\theta + 2\pi/3) \\ \sin\theta & \sin(\theta - 2\pi/3) & \sin(\theta + 2\pi/3) \\ \frac{1}{2} & \frac{1}{2} & \frac{1}{2} \end{bmatrix} \quad (13)$$

And its inverse is: $[T_{qd0}(\theta)]^{-1} =$

$$\begin{bmatrix} cos\theta & sin\theta & 1 \\ \cos(\theta - 2\pi/3) & \sin(\theta - 2\pi/3) & 1 \\ \cos(\theta + 2\pi/3) & \sin(\theta + 2\pi/3) & 1 \end{bmatrix} \quad (14)$$

The equations for the motor current values are obtained from the matrix equation below:

$$\begin{bmatrix}\Psi_{qs}^{s}\\ \Psi_{ds}^{s}\\ \Psi_{0s}\\ \Psi_{qr}^{'s}\\ \Psi_{dr}^{'s}\\ \Psi_{0r}^{'}\end{bmatrix}=\begin{bmatrix}x_{ls}+x_m & 0 & 0 & x_m & 0 & 0\\ 0 & x_{ls}+x_m & 0 & 0 & x_m & 0\\ 0 & 0 & x_{ls} & 0 & 0 & 0\\ x_m & 0 & 0 & x_{lr}'+x_m & 0 & 0\\ 0 & x_m & 0 & 0 & x_{lr}'+x_m & 0\\ 0 & 0 & 0 & 0 & 0 & x_{lr}'\end{bmatrix}\begin{bmatrix}i_{qs}^{s}\\ i_{ds}^{s}\\ i_{0s}\\ i_{qr}^{'s}\\ i_{dr}^{'s}\\ i_{0r}^{'}\end{bmatrix}$$

(15)

The stator abc phase currents can be determined from the stator qd currents using the inverse transformation (Park's transformation), where θ is zero.

$$[I_{abcs}]=[T_{qdo}(\Theta)]^{-1}[I_{qdos}]$$

(16)

$$\begin{bmatrix}i_{as}\\ i_{bs}\\ i_{cs}\end{bmatrix}=\begin{bmatrix}1 & 0 & 1\\ -\frac{1}{2} & -\frac{\sqrt{3}}{2} & 1\\ -\frac{1}{2} & \frac{\sqrt{3}}{2} & 1\end{bmatrix}\begin{bmatrix}i_{qs}^{s}\\ i_{ds}^{s}\\ i_{os}\end{bmatrix}$$

(17)

The rotor abc phase current can be determined from the rotor qd currents using the inverse qd0 to abc transformation with θ=0.

$$[I_{abcr}]=[T_{qdo}(\Theta)]^{-1}[I_{qdor}]$$

(18)

$$\begin{bmatrix}i_{ar}\\ i_{br}\\ i_{cr}\end{bmatrix}=\begin{bmatrix}\cos(w_e t-w_r t) & \sin(w_e t-w_r t) & 1\\ \cos(w_e t-w_r t-2\pi/3) & \sin(w_e t-w_r t-2\pi/3) & 1\\ \cos(w_e t-w_r t+2\pi/3) & \sin(w_e t-w_r t+2\pi/3) & 1\end{bmatrix}\begin{bmatrix}i_{qr}'\\ i_{dr}'\\ i_{0r}'\end{bmatrix}$$

(19)

$$\begin{bmatrix}i_{ar}^{'}\\ i_{br}^{'}\\ i_{cr}^{'}\end{bmatrix}=\begin{bmatrix}1 & 0 & 1\\ -\frac{1}{2} & -\frac{\sqrt{3}}{2} & 1\\ -\frac{1}{2} & \frac{\sqrt{3}}{2} & 1\end{bmatrix}\begin{bmatrix}i_{qr}^{'r}\\ i_{dr}^{'r}\\ i_{0r}^{'}\end{bmatrix}$$

(20)

Also for the stator and rotor voltage abc, we use the park's transformation ratio expression; $[V_{abcs}]=[T_{qdo}(\theta)]^{-1}[V_{qdos}]$ and

$$[V_{abcr}]=[T_{qdo}(\theta)]^{-1}[V_{qdor}]$$

(21)

$$\begin{bmatrix}V_{as}\\ V_{bs}\\ V_{cs}\end{bmatrix}=\begin{bmatrix}1 & 0 & 1\\ -\frac{1}{2} & -\frac{\sqrt{3}}{2} & 1\\ -\frac{1}{2} & \frac{\sqrt{3}}{2} & 1\end{bmatrix}\begin{bmatrix}V_{qs}^{s}\\ V_{ds}^{s}\\ V_{0s}\end{bmatrix}$$

(22)

The model equations of the Three Phase Asynchronous (Induction) Machine in the stationary qd0 reference frame may be rearranged into the following form for the purpose of dynamic simulation.
Q-axis stator flux linkage per second and D-axis stator flux linkage per second

$$\psi_{qs}^{s}=w_b\int\left\{v_{qs}^{s}+\frac{r_s}{x_{ls}}\left(\psi_{mq}^{s}-\psi_{qs}^{s}\right)\right\}dt$$

(23)

$$\psi_{ds}^{s}=w_b\int\left\{v_{ds}^{s}+\frac{r_s}{x_{ls}}\left(\psi_{md}^{s}-\psi_{ds}^{s}\right)\right\}dt$$

(24)

Zero sequence stator current

$$i_{0s}=\frac{w_b}{x_{ls}}\int(v_{0s}-i_{0s}r_s)\,dt$$

(25)

Q-axis referred rotor flux linkage per second and D-axis referred rotor flux linkage per second

$$\psi_{qr}^{'s}=w_b\int\left\{v_{qr}^{'s}+\frac{w_r}{w_b}\psi_{dr}^{'s}+\frac{r_r^{'}}{x_{ls}^{'}}\left(\psi_{mq}^{s}-\psi_{qr}^{'s}\right)\right\}dt$$

(26)

$$\psi_{dr}^{'s}=w_b\int\left\{v_{dr}^{'s}-\frac{w_r}{w_b}\psi_{qr}^{'s}+\frac{r_r^{'}}{x_{lr}^{'}}\left(\psi_{md}^{s}-\psi_{dr}^{'s}\right)\right\}dt$$

(27)

Zero sequence referred rotor current

$$i_{0r}^{'}=\frac{w_b}{x_{lr}^{'}}\int\left(v_{0r}^{'}-i_{0r}^{'}r_r^{'}\right)dt$$

(28)

Q-axis magnetizing flux linkage per second and D-axis magnetizing flux linkage per second

$$\psi_{mq}^{s}=x_m\left(i_{qs}^{s}+i_{qr}^{'s}\right)\text{and}\ \psi_{md}^{s}=x_m\left(i_{ds}^{s}+i_{dr}^{'s}\right)$$

(29)

Q-axis stator flux linkage per second and D-axis stator flux linkage per second $\psi_{qs}^{s}=x_{ls}i_{qs}^{s}+\psi_{mq}^{s}$ and

$$\psi_{ds}^{s}=x_{ls}i_{ds}^{s}+\psi_{md}^{s}$$

(30)

Q-axis referred rotor flux linkage per second and D-axis referred rotor flux linkage per second

$$\psi_{qr}^{'s}=x_{ir}^{'}i_{qr}^{'s}+\psi_{mq}^{s}\ \text{and}\ \psi_{dr}^{'s}=x_{ir}^{'}i_{dr}^{'s}+\psi_{md}^{s}$$

(31)

Q-axis stator current and D-axis stator current

$$i_{qs}^{s}=\frac{\psi_{qs}^{s}-\psi_{mq}^{s}}{x_{ls}}\ \text{and}\ i_{ds}^{s}=\frac{\psi_{ds}^{s}-\psi_{md}^{s}}{x_{ls}}$$

(32)

Q-axis referred rotor current and D-axis referred rotor current

$$i_{qr}^{'s}=\frac{\psi_{qr}^{'s}-\psi_{md}^{s}}{x_{lr}^{'}}\ \text{and}\ i_{dr}^{'s}=\frac{\psi_{dr}^{'s}-\psi_{md}^{s}}{x_{lr}^{'}}$$

(33)

And

$$\psi_{mq}^{s}=x_M\left(\frac{\psi_{qs}^{s}}{x_{ls}}+\frac{\psi_{qr}^{'s}}{x_{lr}^{'}}\right)\ \text{while}\ \psi_{md}^{s}=x_M\left(\frac{\psi_{ds}^{s}}{x_{ls}}+\frac{\psi_{dr}^{'s}}{x_{lr}^{'}}\right)$$

(34)

The Torque equation is given by:

$$T_{em}=\frac{3}{2}*\frac{P}{2w_b}\left(\Psi_{ds}^{s}i_{qs}^{s}-\Psi_{qs}^{s}i_{ds}^{s}\right)\qquad N.m$$

(35)

The relationship between torque and motor speed is given below as:

$$\frac{2J}{P} * \frac{dw_r}{dt} = T_{em} + T_{mech} - T_{damp} \qquad N.m. \quad (36)$$

Where: w_b =base speed; w_r = rotor speed; r_s = stator resistance; x_{ls} = stator reactance; $r_r^{'}$ = rotor referred resistance; x_{lr} = rotor referred reactance; x_m = magnetizing reactance; x_M = machine equivalent star reactance; T_{em} = electromechanical torque; T_{mech} = externally applied mechanical load torque; T_{damp} = damping torque; J= combined moment of inertia; v_{qs}^{s} = q-axis stator voltage; v_{ds}^{s} = d-axis stator voltage; $v_{qr}^{'s}$ = q-axis referred rotor voltage; $v_{dr}^{'s}$ = d-axis referred rotor voltage; v_{0s} = zero sequence stator voltage; v_{0r} = zero sequence rotor voltage.

3.2. Motor parameter

The three phase induction motor parameters used for this study are presented in table 1 below. It is a 4-pole, 60-Hz, 3-phase induction motor, and its parameters are expressed in ohms using the 60Hz value of the reactances.

Table 1: Machine Parameters

Parameter	Value
Rated Power	500 hp
Rated phase voltage	230V
Rated Speed	1773rpm
Rated Torque	1980Nm
Nominal current	93.6A
Stator resistance per phase, r_s	0.262 Ω
Stator leakage reactance per phase, X_{ls}	1.206 Ω
Magnetizing reactance, X_m	54.02 Ω
Rotor leakage reactance referred to the stator, $X_{lr}^{'}$	1.206 Ω
Rotor resistance referred to the stator, $r_r^{'}$	0.187 Ω
Moment of Inertia (J)	11.06 Kg.m^2

4. Direct on-line starting (DOL)

In this starting scheme, the induction motor was started directly without starter of any sort. The stator coils were connected in delta. The motor was loaded with the rated torque of 1980Nm at 2 seconds after start-up. Below is the SIMULINK model and the simulation results.

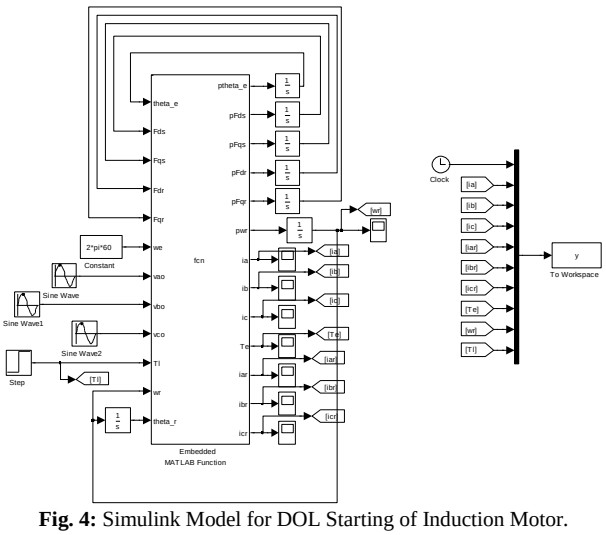

Fig. 4: Simulink Model for DOL Starting of Induction Motor.

5. Results of direct on-line starting

The following results were obtained for this simulation

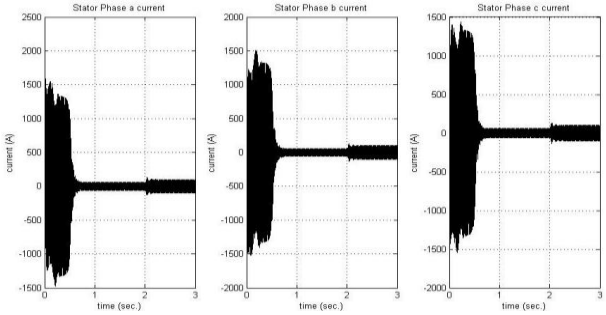

Fig. 5: Stator Currents in the Three Phases.

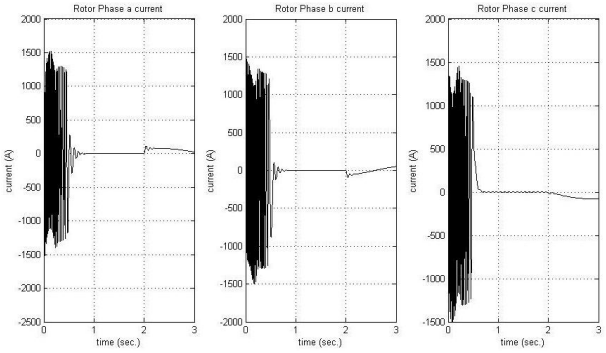

Fig. 6: Rotor Currents in the Three Phases.

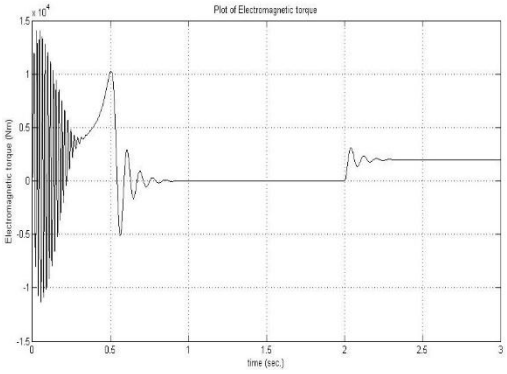

Fig. 7: Plot of Electromagnetic Torque.

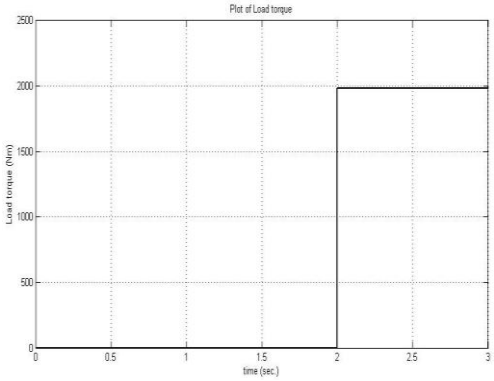

Fig. 8: Plot of Load Torque.

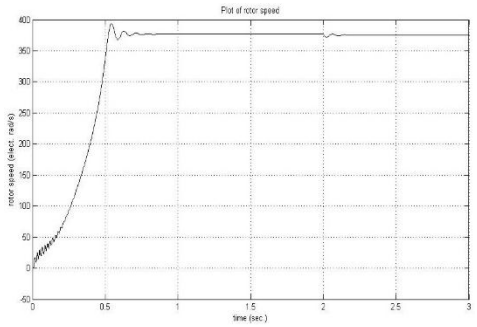

Fig. 9: Plot of Rotor Speed.

4.1. Discussion of results

Figure 5 shows starting phase current amplitude of up to 1500A for the DOL starter. Such high starting current can cause instability to the power system and may result to voltage sagging. A star-delta starter would have about fifty percent (50%) reduction and may not cause as much instability.

The rotor current for the DOL is presented in figure 6. The rotor starting current is about the same magnitude with that of the stator current because of transformer action and also because it is referred value to the stator. After the start-up the frequency of the rotor current becomes relatively low because the speed of the motor is now close to the synchronous speed. At the time interval when the motor is moving at synchronous speed it can be seen that the rotor currents are all equal to zero.

The electromagnetic torque for the DOL is presented in figure 7. The motor shows a pulsating torque during start-up, but on the average, this torque is positive and helps to overcome the inertia torque. When the load is applied, the motor reacts to produce an almost steady torque after a while to overcome the load torque.

Figure 9 shows the motor speed for the DOL. Whenever the motor is loaded the speed drops and if it is unloaded the speed increases, though not so obvious in this figure. The reason for this is because when the induction motor is loaded, its speed drops so that more emf will be induced in the rotor, consequently more current and torque would be produced to counter this load.

From the simulation results of the balanced load, the phase currents are relatively of very low harmonics compared to its unbalanced state.

Also from the result, it was observed that an induction motor under balanced load (voltages) will result in decreased heating at rated horsepower load hence would have better thermal performance.

6. Conclusion

This investigation has shown that for readers that are conversant with the Star – Delta starting scheme, there is an appreciable difference in the performance of an induction motor under balance load in this case of DOL starting scheme. The induction motor differences in operational characteristics for the DOL in comparison with the Star-Delta show that they are not very similar during transients and start-up periods but remain the same thereafter. The overall results are very useful for the industry, machine designers and academia in general.

References

[1] S.K. Bhattacharya, Electrical Machines, Tata Mc Graw-Hill publishing company Ltd, New Delhi, Second edition, 1998, page 287.

[2] M.C. Richard, "Electrical Drives and their control". Oxford University Press: New York, 1995.

[3] P.C. Krause, O. Wasynczuk and S.D. Sandolf "Analysis of Electric Machinery and Drive System, IEEE press, Wiley & sons Publishers, second edition, 2002. https://doi.org/10.1109/9780470544167.

[4] O.I. Okoro, "Dynamic Modelling and Simulation of Squirrel-Cage Asynchronous Machine with Non-Linear Effects". Journal of ASTM International. 2(6), 2005, 1-16. https://doi.org/10.1520/JAI14018.

[5] N.S. Nyein, "Dynamic Modelling and Simulation of $3-\phi$ Small Power Induction Motor". International World Academy of Science, Engineering and Technology, 2000, pp. 18.

[6] E.J. Akpama, O.I. Okoro., and E. Chikuni, "Simulation of the Performance of Induction Machine under Unbalanced Source Voltage Conditions". Pacific Journal of Science and Technology. 11(1), 2010, pp. 9-15.

[7] M. Batool. "Mathematical Modelling and Speed Torque Analysis of $3-\phi$ Induction Motor using MATLAB". Second Edition, McGraw Hill, 1995; pp. 9-17.

[8] C.O. Nwankpa. 2005. "Induction Motor tests using MATLAB". IEEE Transactions on Education, Vol. 48, 2005, pp. 1.

[9] O.I. Okoro., 'Dynamic and Thermal modelling of Induction machine with Non-Linear Effects', Ph.D. Thesis, University of Kassel Press, Germany, September 2002.

[10] Ching-Yin Lee. 1999. "Effects of unbalance voltage on the operation performance of Three Phase Induction Motor". IEEE Trans. on Energy Conversion. 14:202-208. https://doi.org/10.1109/60.766984.

[11] Faiz, J. 2004. "Influence of unbalanced voltage on the steady-state performance of $3-\phi$ Squirrel-cage Induction Machine". IEEE Trans. Energy conversion. 19(4):657-662. https://doi.org/10.1109/TEC.2004.837283.

[12] Pillay, P., Hofmann, P., M. Manyage. 2002. "De-rating of Induction Motor operating with a combination of unbalanced voltages and under voltages". IEEE Trans. Energy conversion. 17(4):485-491. https://doi.org/10.1109/TEC.2002.805228.

[13] Chee Mun Ong. "Dynamic Simulation of Electric Machinery using Matlab/Simulink". Upper Saddle River, New Jersey, 1997, pp. 229.